

Damping and Trapping in 2D Inviscid Fluids

N. Sateesh Pillai and Roy W. Gould

California Institute of Technology, Pasadena, California 91125

(Received 6 July 1993; revised manuscript received 11 August 1994)

We demonstrate collisionless decay due to phase mixing of a disturbance in an inviscid 2D fluid with sheared flow. Experiments performed on a cylindrical pure electron plasma, which behaves as a 2D inviscid fluid, show that a small amplitude quadrupole excitation ($m = 2$, $k = 0$ mode) decays exponentially. At larger amplitudes, the exponential decay is modulated by bounce motion of fluid elements trapped in the azimuthally traveling wave field, with the bounce frequency proportional to the square root of the excitation amplitude. We also show that the linear decay rate is *decreased* by the addition of external dissipation. We describe a calculation of the linearized response function.

PACS numbers: 47.15.Ki, 52.25.Wz, 52.35.Lv, 52.35.Mw

Two-dimensional flow of incompressible inviscid fluids has a long history [1–3]. The 2D behavior of non-neutral plasmas, in the drift approximation, is analogous to that of inviscid fluids [4,5], with equipotentials as fluid streamlines and plasma density proportional to vorticity. Very recently this property has been exploited to study several classic problems in 2D vortex dynamics [5–8]. In sheared 2D flows, disturbances are convected in different layers with different velocities, and this is predicted to lead to collisionless decay of disturbances due to phase mixing. For example, using an initial value approach, Case [3] showed theoretically that in planar Couette flow of an inviscid fluid, small perturbations decay algebraically in the asymptotic limit. Briggs *et al.* [4], in a theoretical study, also argued that small 2D perturbations in a cylindrical non-neutral plasma column with sheared flow are expected to decay due to a collisionless phase mixing process similar to Landau damping of Langmuir oscillations [9]. deGrassie [10] was the first to search for this phenomena experimentally. Although he found the perturbations decayed, the decay rates obtained were about 2 orders of magnitude smaller than expected, and they decreased with increasing amplitude of excitation, i.e., a *nonlinear* behavior. The sensitivity of his receiver was inadequate to observe the linear regime.

We present three new experimental results on vortex dynamics. (a) We observe collisionless damping of 2D disturbances of the form $\exp[im\theta + ikz - i\omega t]$, with $m = 2$ and $k = 0$, in an inviscid fluid in the *linear* regime. (b) We find that as the amplitude of excitation is increased, the decay rate is modulated periodically in a manner consistent with bounce motion of trapped fluid elements in the field of the disturbance. This is in accordance with the early picture of Kelvin's cat's eyes [2] and a prediction of Briggs *et al.* [4] that the bounce frequency should be proportional to the square root of the perturbed amplitude. This phenomenon is qualitatively similar to the effect of bounce oscillations of particles trapped by a Langmuir mode [11–13]. (c) We show that adding external dissipation to the system *reduces* the

linear damping rate, thus demonstrating that the mode has *negative energy*, i.e., excitation of the mode reduces the energy of the system.

We also describe a calculation of the linear response function of a 2D cylindrical fluid which exhibits exponential decay at early times, associated with a simple pole, followed by a transition to algebraic decay, similar to the asymptotic prediction of Case [3]. This response function also shows that the mode has *negative energy*.

Our experiments were performed using a cylindrical pure electron plasma column illustrated in Fig. 1(a). Electrons emitted from a hot thoriated tungsten filament are injected into the trap region where they are confined in the radial direction by a 50 G magnetic field and in the axial direction by electrostatic traps held at -100 V. The trapped electrons will rotate around the cylinder axis under steady state. A radial monotonically

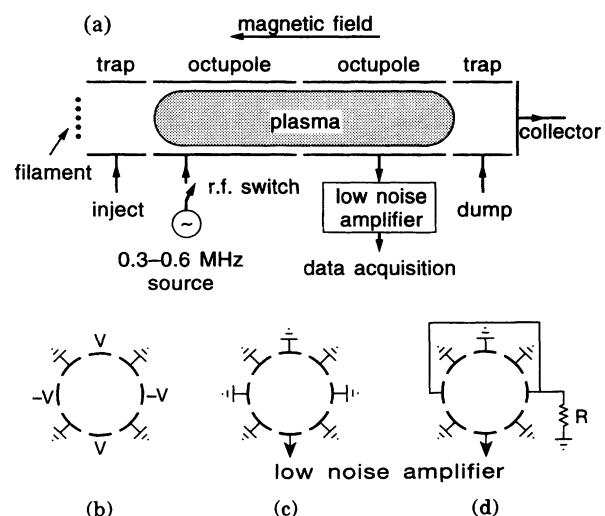


FIG. 1. (a) Schematic of cylindrical structure for plasma trapping and excitation. (b) phasing of first octupole for exciting an $m = 2$ disturbance, (c) configuration of second octupole for signal reception, and (d) configuration of second octupole for negative energy test.

decreasing particle density profile (vorticity profile in fluid terms) produces a monotonically decreasing angular velocity of fluid rotation, i.e., sheared flow. The plasma radius and lengths are 1.2 and 40 cm, respectively. The cyclotron frequency, central plasma, and rotation frequencies are about 140 MHz, 10 MHz, and 350 kHz, respectively. The Reynolds number is estimated to be 10^4 . Other aspects of this device have been described earlier [14]. The experiment is performed in a repetitive inject-observe-dump cycle. The trapped plasma is excited by a 5 μ sec burst of 300 to 600 kHz sinusoid on one octupole set. The frequency of the rf pulse is adjusted so as to maximize the response of the $m = 2$ mode, typically 2–4 times the frequency of the well studied $m = 1$ diocotron mode [9]. As shown in Fig. 1(b), signal phases on the octupole sectors generate an $m = 2$ field. The charge induced on one sector of a second octupole section is amplified by a low noise charge amplifier and digitized. The response to the short burst, after it has ended, is a decaying sinusoid as shown in the inset of Fig. 2. Each digitized signal is processed by passing it through a software peak detector to obtain the envelope of the decaying sinusoid. The envelopes of 20 decays (typically) at the same amplitude are averaged and the process repeated for applied voltage between 10 mV to 1 V. The averaged envelopes are shown on a semilogarithmic plot in Fig. 2. For clarity, the traces in the plot are stopped when the signal becomes comparable with the system noise level. The lowest four traces in Fig. 2 evidently represent the linear regime, since the response is simply proportional to the applied voltage. The linear decay rate is $\gamma = 34.3$ krad/sec and $\omega/\gamma = 84$. The

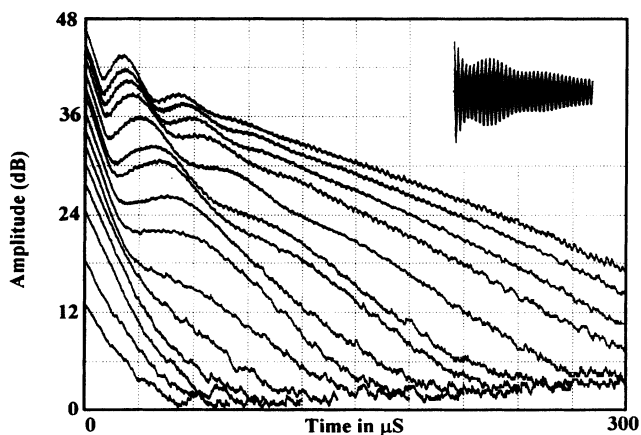


FIG. 2. Decay of the envelope of $m = 2$ signal at about 400 kHz, excited by an rf pulse with voltages 10, 20, 40, 60, 80, 120, 160, 200, 250, 300, 400, 500, 600, 700, and 1000 mV. Lower left curve corresponds to 10 mV rf voltage and uppermost curve corresponds to 1000 mV. Plotted on semilogarithmic scale with vertical scale calibrated in dB. Time scale starts with $t = 0$ at the end of the rf pulse. Inset shows received signal for 500 mV applied voltage.

decay time in the linear regime is much shorter than the electron-electron collision time of 10 msec. Hence this decay is *collisionless*. The *initial* decay rates for *all traces* during the first 15 μ sec are approximately the same. Later in time and at higher amplitudes, the decay rate is periodically modulated, with the shortest modulation period occurring at the highest amplitude. At the lower amplitudes, the modulation period becomes larger than the decay time and the nonlinear modulation phenomenon disappears. At these low amplitudes, a fluid element cannot complete a trapped orbit before the mode decays and, in effect, does not know that it is trapped. At higher amplitudes a fluid element is able to complete a trapped orbit before the mode decays and the modulation of the wave amplitude becomes noticeable. The smallest observable bounce frequency, 94.3 krad/sec, is larger than the linear decay rate. At the largest amplitudes, the late-time decay is much slower, and we find a nonlinear behavior in which the decay rate decreases with increasing amplitude, similar to that described by deGrassie [10].

In order to determine the dependence of the bounce period on the mode potential we have analyzed the data of Fig. 2 in the following way. First, we determine a least squares exponential fit to the early part of one of the traces to get the average rate of decay. We then subtract this exponential from that trace and determine the bounce period by measuring the time between successive maxima. We observe that the period lengthens as the mode decays, as expected. We correct the mode potential for this decay using the exponential function and, assuming the initial mode potential to be proportional to the applied voltage, plot the resulting bounce frequency versus the corrected *applied* potential. Figure 3 shows the resulting bounce frequency f versus V on a log-log plot. A least squares fit of the form $f = AV^n$ to the data, shown by the solid line, gives $n = 0.44$ and $A = 2.77$ (f in kHz and V in mV). Calculations for 21 other data sets, similar to those shown in Figs. 2 and 3, give values of n between 0.42 and 0.77 with a mean value of 0.55 ± 0.10 . This is equal, within experimental error, to the value of 0.5 expected for oscillations of trapped particles in the mode [4], and reinforces our conclusion that the amplitude modulation of the decaying $m = 2$ mode is due to fluid trapping at a radius where the local angular velocity is equal to the mode velocity.

We now sketch the theoretical calculation of the linear response function of the system associated with a single m value, namely $m = 2$. The response of the plasma to a burst of sinusoid of amplitude V is induced current I in the wall of the electrode (Fig. 1). In the linear regime, the Fourier transform of I is related to the Fourier transform of V through a *transfer admittance* $Y(\omega)$: $I(\omega) = V(\omega)Y(\omega)$. It is easy to show that $Y(\omega) = i\omega 2\pi\epsilon_0 L F_1 F_2 (rE_r/\phi)_{r=b}$, where L is the total length of the trap, F_1 and F_2 are geometrical form

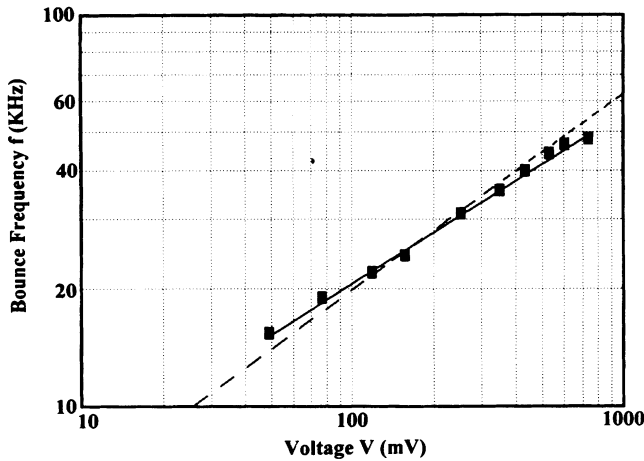


FIG. 3. Bounce frequency f versus voltage V (applied voltage corrected for the decay) plotted on a log-log scale. Filled boxes correspond to data. Solid line is a least squares fit $f = AV^n$, where $n = 0.44$. Together with 21 other data sets, $n = 0.55 \pm 0.1$. Dashed line shows a line where $n = 0.5$ for comparison.

factors (<1) pertaining to length, mode number m , and phasing of the sectors of the input and output octupole sections. E_r/ϕ represents the ratio of the radial electric field to the potential and should be evaluated at the wall ($r = b$). $Y(\omega)$ is just the Fourier transform of the impulse response of the plasma. The value of E_r/ϕ at the wall can be obtained by solving the linearized equation for the potential [4,5]:

$$\frac{d^2 \phi}{dr^2} + \frac{1}{r} \frac{d\phi}{dr} - \frac{m^2}{r^2} \phi + \frac{me}{\epsilon_0 B_0} \frac{dn_0(r)/dr}{r[\omega - m\omega_0(r)]} \phi = 0, \tag{1}$$

where $n_0(r)$ represents the particle density and $\omega_0(r)$ the angular velocity of electrons of charge e confined in a magnetic field B_0 . For a band of ω 's a mode particle resonance will occur at a radius r_s within the plasma where $m\omega_0(r_s) = \omega$, giving rise to a logarithmic singularity in ϕ at $r = r_s$. To solve Eq. (1) requires a knowledge of $n_0(r)$ from which $\omega_0(r)$ is determined. Power series expressions have been obtained for special profile functions, but for a greater variety of profiles we also integrate Eq. (1) numerically for various ω . In order to deal with the singularity at $r = r_s$ in the solution of Eq. (1), ω is assumed to have a small positive imaginary part. Using this technique we obtain the frequency-dependent real and imaginary parts of $(rE_r/\phi)_b$ that are shown in Fig. 4(a). The corresponding envelope of the impulse response is obtained by taking the inverse Fourier transform of $(rE_r/\phi)_b$ and is shown in Fig. 4(b). $(rE_r/\phi)_b$ can be fit rather well by the expression for a simple pole, plus a small remainder function $\Re(\omega)$, which accounts for the asymmetry: $Y(\omega) = i\omega B/(\omega - \omega_2 + i\gamma_2) + \Re(\omega)$ ($\gamma_2 > 0$). The pole lies in the lower half

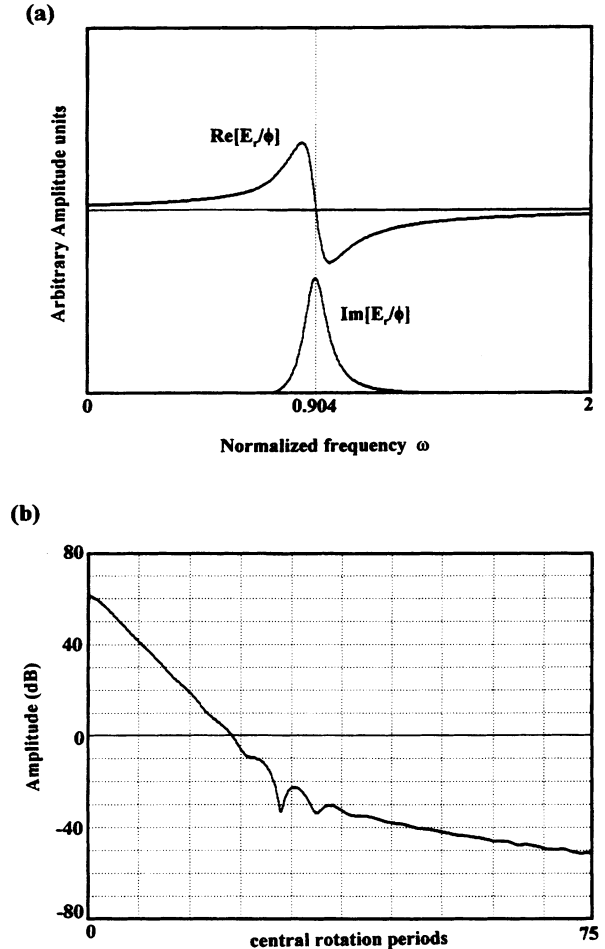


FIG. 4. (a) Real and imaginary parts of $(rE_r/\phi)_{r=b}$ as a function of frequency ω for the $m = 2$. Central angular velocity corresponds to $\omega = 2$, and angular velocity at the wall ($r = b$) corresponds to $\omega = 0.714$ for $m = 2$. The dotted vertical line in the middle corresponds to the theoretical prediction of the $m = 2$ resonant frequency $\omega = 0.904$ for this profile. (b) Semilogarithmic plot of the envelope of inverse Fourier transform of $(rE_r/\phi)_{r=b}$. Initial exponential decay change to an asymptotic algebraic decay with some interference in between.

frequency plane, a location which can only be reached by analytic continuation of our solution of Eq. (1), and is responsible for the early exponential decay (with rate γ_2) seen in Fig. 4(b). The precise way in which $\text{Re}\{Y(\omega)\}$ goes to zero depends upon the way in which the density $n_0(r)$ goes to zero at the plasma edge, and this also determines the form of the algebraic decay in asymptotic limit of the impulse response. The Q of the resonance $\omega_2/2\gamma_2$ and the frequency ω_2 , relative to the central rotation frequency, depends on details of the density profile. Some profiles exhibit a Q close to the experimentally observed value of 84. The form of $Y(\omega)$

is qualitatively similar for the various density profiles and modes that we have studied numerically.

An important feature of the admittance calculation is that the constant B is *negative*, opposite from that expected for passive systems (e.g., a tuned RLC circuit). Neutrally stable (undamped) negative energy modes are destabilized by removal of energy through dissipation. This has been well documented for the $m = 1$ diocotron mode [15]. In our case, the $m = 2$ mode is already damped, though not by dissipation but one might expect that the addition of dissipation would *reduce* the damping rate and perhaps even turn it into a growing mode. Using the admittance function one can show that a resistive or dissipative boundary condition at the outer edge of the plasma *reduces* the growth rate. When a resistor R is placed in parallel with the octupole section, as in Fig. 1(d), the following equation holds: $Y(\omega) + (1/R) = 0$. Using the simple pole approximation and neglecting the small remainder function $\Re(\omega)$ we obtain for mode frequency $\omega = \omega_2 - i(\gamma_2 + \omega_2 BR)$. The last term shows that when $B < 0$ there should be a *reduction* in the damping rate of the mode proportional to the resistance R , whereas when $B > 0$ the damping rate is *increased*.

External dissipation is easily added experimentally by connecting resistors to unused segments of the octupole sections. Two precautions are necessary. First, the resistors must be connected so as to affect the $m = 2$ mode but not the $m = 1$ mode, because the latter would be immediately destabilized. This is accomplished connecting the resistor simultaneously to two diametrically opposite segments of an octupole, as shown in Fig. 1(d). Second, the cable capacitance must be "tuned out" by adding a parallel inductor, selected so that parallel resonant frequency is equal to the frequency of the $m = 2$ mode. Experimentally it is found that the connection of an external resistor to the wall electrodes in this fashion causes the damping rate to *decrease* rather than increase and with high enough resistance; the mode is seen to be destabilized. The reduction in decay rate by external dissipation is shown in Fig. 5. Theoretically, since the form of $Y(\omega)$ is similar for higher modes also, one expects similar behavior for the $m = 3$ and higher modes.

In summary, our experimental observations reveal, for the first time, three important characteristics of an $m = 2$ fluid perturbation. First is collisionless damping of small perturbations with evidence for a dominant pole which follows from the observed exponential decay of the linear

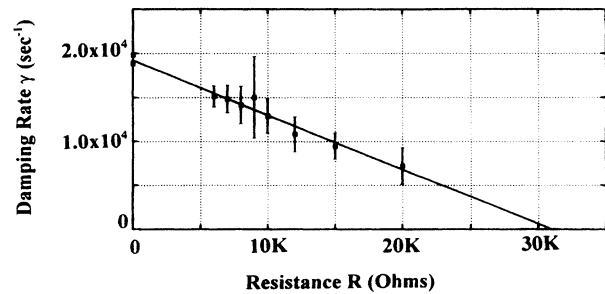


FIG. 5. Decay rate of the $m = 2$ response versus resistance when a resistor is connected to the wall electrode. Line is a least squares fit of the experimental data obtained from a large number of responses.

response. Second is evidence at large amplitudes for fluid trapping by the mode, with a bounce frequency proportional to the square root of the amplitude. Third, the decaying disturbance has negative energy and decays less rapidly when external dissipation is added.

This work was supported by ONR Grant No. N00014-89-J-1264.

- [1] J. W. S. Rayleigh, Proc. London Math. Soc. **11**, 57 (1880).
- [2] W. Thomson, Nature (London) **23**, 45 (1880).
- [3] K. M. Case, Phys. Fluids **3**, 143 (1960).
- [4] R. J. Briggs, J. D. Daugherty, and R. H. Levy, Phys. Fluids **13**, 421 (1970).
- [5] C. F. Driscoll and K. S. Fine, Phys. Fluids B **2**, 1359 (1990).
- [6] A. J. Peurrung and J. Fajans, Phys. Fluids A **5**, 493 (1993).
- [7] T. B. Mitchell, C. F. Driscoll, and K. S. Fine, Phys. Rev. Lett. **71**, 1371 (1993).
- [8] X.-P. Huang and C. F. Driscoll, Phys. Rev. Lett. **72**, 2187 (1994).
- [9] L. Landau, J. Phys. (Moscow) **10**, 25 (1946).
- [10] J. S. deGrassie and J. H. Malmberg, Phys. Rev. Lett. **39**, 1077 (1977); Phys. Fluids **23**, 63 (1980).
- [11] T. M. O'Neil, Phys. Fluids **8**, 2255 (1965).
- [12] J. H. Malmberg and C. B. Wharton, Phys. Rev. Lett. **19**, 775 (1967).
- [13] C. B. Wharton, J. H. Malmberg, and T. M. O'Neil, Phys. Fluids **11**, 1761 (1968).
- [14] R. W. Gould and M. A. LaPointe, Phys. Rev. Lett. **67**, 3685 (1991); R. W. Gould and M. A. LaPointe, Phys. Fluids B **4**, 2038 (1992).
- [15] W. D. White, J. H. Malmberg, and C. F. Driscoll, Phys. Rev. Lett. **49**, 1822 (1982).

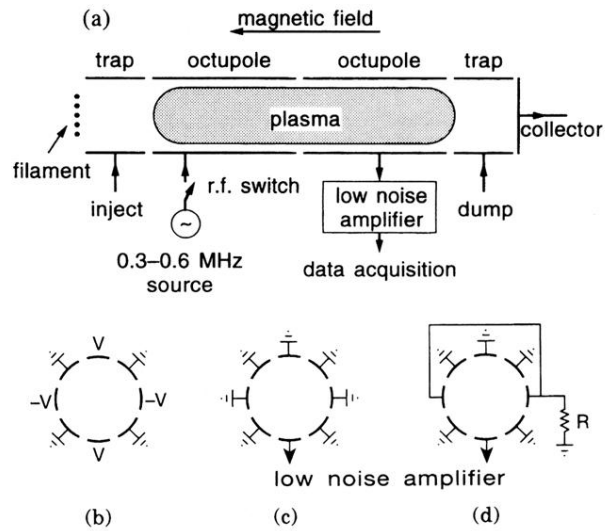


FIG. 1. (a) Schematic of cylindrical structure for plasma trapping and excitation. (b) phasing of first octupole for exciting an $m = 2$ disturbance, (c) configuration of second octupole for signal reception, and (d) configuration of second octupole for negative energy test.